

SPECTRAL INDICATIONS OF DENSITY VARIABILITY IN THE CORONA OF AD LEONIS

A. MAGGIO¹, J.-U. NESS²
Draft version November 10, 2018

ABSTRACT

Direct comparison of high-resolution X-ray spectra of the active dMe star AD Leo, observed three times with *Chandra*, shows variability of key density-sensitive lines, possibly due to flaring activity. In particular, a significant long-duration enhancement of the coronal density is indicated by the Ne IX and Si XIII He-like triplets, and possibly also by density-sensitive Fe XXI line ratios.

Subject headings: stars: individual (AD Leo) — stars: activity — stars: coronae — stars: late-type — X-rays: stars

1. INTRODUCTION

The plasma density is a crucial parameter for understanding the structure of stellar coronae. Rather than being uniformly distributed on large spatial scales, as occurs in the photosphere, the coronal plasma is trapped by surface magnetic fields within scale lengths typically much smaller than the stellar radius, and is likely to be very inhomogeneous in density. The patchy appearance of the solar corona in X-rays is mainly a density effect; since the radiative emission of an optically thin plasma excited by collisional excitation is proportional to the square density, the observed irradiance traces preferentially high-density “compact” regions, confined by small-scale magnetic fields. The plasma density is also expected to vary in time owing to the dynamics of these fields and of the plasma itself; in particular, the coronal density is expected to increase *locally* as a consequence of impulsive heating events (flares) which trigger an upward motion of denser plasma from deeper atmospheric layers (“chromospheric evaporation”).

The measurement of plasma densities in stellar coronae is a relatively recent practice in X-ray spectroscopy; *Chandra* and XMM-Newton high-resolution gratings provide us with a number of density-sensitive emission lines, which are now routinely employed to this purpose. However, density estimates and their interpretation are more difficult and challenging than expected, for several reasons; first, even in relatively strong X-ray sources the relevant emission lines may be difficult to measure owing to low ion abundances, severe blends with other spectral features, or insufficient instrumental sensitivity in the relevant wavelength ranges; secondly, different spectral diagnostics probe coronal regions at different temperatures, and they often yield density estimates which are difficult to reconcile; finally, the lack of spatial resolution in observations of stellar coronae allows us to obtain only “effective” densities, averaged over all the coronal structures in the visible hemisphere and weighted by the plasma irradiance, so that any interpretation becomes model dependent.

For the above reasons, it is currently easier to look for variations with time in the plasma density in a given coronal source, rather than comparing absolute values derived from snapshots of different stars. In this respect, energetic events

like stellar flares are natural experiments to examine, and they have been the subject of several investigations in recent years; nonetheless, convincing evidence of density variations are scanty in the literature, with notable exceptions such as the flare recently observed in the nearby dMe star Proxima Centauri (Güdel et al. 2002).

In this paper we present the first evidence of significant long-term density variations in the corona of AD Leo, another well-known dMe flare star observed several times with the *Chandra* X-ray Observatory (Weisskopf et al. 2002). The strength of the present evidence comes from the direct comparison of high-resolution X-ray spectra taken at different times, with little need of data adjustments or problematic atomic models. On the other hand, the interpretation of the results is unclear, but gives some new hints on issues under debate in stellar X-ray spectroscopy and coronal physics.

2. TARGET AND OBSERVATIONS

AD Leo is one of the X-ray brightest single dMe stars currently known, having quite a stable quiescent X-ray luminosity, $L_x = 3\text{--}5 \times 10^{28}$ erg s⁻¹ (0.5–4.5 keV band) over a 17 yr period, as determined by Favata et al. (2000a). On the other hand, it is also a quite variable X-ray source on short time scales, owing to its characteristic coronal magnetic activity (see e.g. Audard et al. 2000).

AD Leo was observed twice with the *Chandra* Low-Energy Transmission Grating Spectrometer (LETGS) in January and October 2000, as part of the GTO program, and once again in June 2002 with the High-Energy Transmission Grating Spectrometers (HETGS). A detailed analysis of the October 2000 observation was presented by Maggio et al. (2004), including a reconstruction of the plasma emission measure distribution (EMD) with temperature, and evaluation of the plasma densities at various temperatures by means of the He-like triplets and Fe XXI lines. Here we will focus on the comparison of this observation with the previous one, since they have about the same exposure time (48 ks and 46 ks, respectively), and we will also briefly discuss results based on the shorter Jan 2000 observation (10 ks).

The data were retrieved from the *Chandra* archive and reprocessed with the *Chandra* Interactive Analysis of Observations (CIAO V3.1) software. We used the tool FULLGARF to calculate effective detector areas. From each observation we have extracted either the LETGS spectrum (6–140 Å), or both the first-order Medium-Energy Grating (MEG, 1–25 Å) and High-Energy Grating (HEG, 1–18 Å) spectra, simultaneously provided by the HETGS; photons from the two dispersion di-

¹ INAF – Osservatorio Astronomico di Palermo, Piazza del Parlamento 1, I-90134 Palermo, Italy; maggio@astropa.unipa.it.

² Department of Physics, Rudolf Peierls Centre for Theoretical Physics, University of Oxford, 1 Keble Road, Oxford OX1 3NP; ness@thphys.ox.ac.uk

rections were coadded to maximize the S/N ratio. We also extracted the spectra in consecutive time bins in order to create the light curves, as described in the following section.

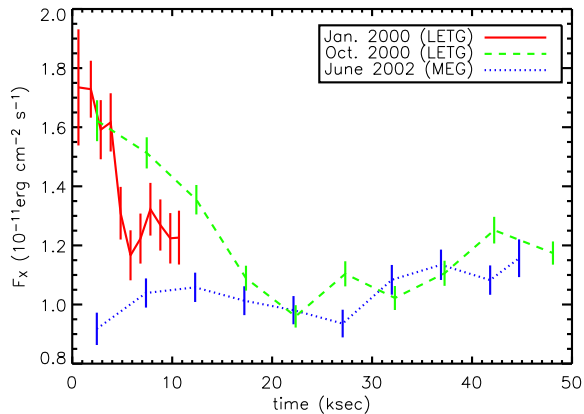


FIG. 1.— AD Leo X-ray light curves (net observed flux in the 7–25 Å wavelength range) derived from the *Chandra* observations reported in the legend. The fluxes were computed by integrating the dispersed spectra extracted in equal time bins, within each observation.

3. ANALYSIS AND RESULTS

3.1. X-ray light curve

Figure 1 shows the X-ray light curves obtained from the three *Chandra* observations: dispersed spectra were extracted from successive time intervals of equal duration, and total X-ray fluxes were computed in the common wavelength range 7–25 Å, after background subtraction and correction for the instrument effective area

No strong isolated flare is visible during these observations, but the Jan and Oct 2000 light curves both show an initial emission level higher than the quiescent one ($f_x \approx 10^{-11}$ erg cm^{-2} s^{-1}) by a factor $\lesssim 2$, followed by a clear decline; this behavior resembles the decay phase of a flare, but we note that in the Oct 2000 light curve the decline is much slower than the expected exponential rate. The latter observation was recently studied by van den Besselaar et al. (2003), who performed a separate analysis of the first 12 ks segment and concluded that the high-temperature tail of EMD was enhanced with respect to the following time segment; on the other hand, Maggio et al. (2004) argue that a rotational modulation effect cannot be completely excluded because the duration of the October 2000 observation is a sizable fraction ($\sim 20\%$) of the photometric rotational period ($P_{\text{rot}} = 2.7$ d, Spiesman & Hawley 1986).

3.2. Analysis and Comparison of Spectra

We have focused our attention on the spectral ranges including the Si XIII, Mg XI, Ne IX, and O VII He-like triplets, and on selected density-sensitive Fe XXI lines. Note that the first three triplets are visible in all LETGS and HETGS spectra, while the O VII triplet can be observed only with the LETGS and the HETGS/MEG. With regard to the Fe XXI lines, we have considered both $2s^22p3d$ transitions to the $2s^22p^2$ ground state which fall at wavelengths in the range 12.28–12.53 Å, and transitions from $2s2p^3$ states which are visible at wavelengths 102.2–145.7 Å only in LETGS spectra (Ness et al. 2004, for more details).

TABLE 1
DENSITY-SENSITIVE FE XXI LINES

λ [Å]	$\log N_e^c$ [cm^{-3}]	Counts	A_{eff} [cm^2]	ISM $e^{-\tau}$	$\lambda/128.73$ line ratio	$\log N_e$ [cm^{-3}]
97.88	12.0 \uparrow	< 10	7.08	0.91	< 0.13	< 12.3
102.22	12.0 \uparrow	18 ± 8	6.71	0.90	0.19 ± 0.10	< 12.3
117.51	13.5 \downarrow	< 8	6.17	0.85	< 0.13	< 11
121.21	12.4 \uparrow	22 ± 9	5.57	0.84	0.30 ± 0.15	12.0–12.9
128.73	12.7 \downarrow	46 ± 11	3.67	0.81		
142.16	12.7 \uparrow	< 15	3.87	0.76	< 0.43	< 13.0
145.65	12.5 \uparrow	15 ± 9	3.69	0.75	0.35 ± 0.23	12.0–13.1

NOTE. — Col 1: theoretical wavelength. Col 2: critical density, and arrow indicating the emissivity trend for increasing N_e . Col 3: observed counts or upper limits. Col 4: LETGS effective area. Col 5: ISM absorption factor, assuming $N_{\text{H}} = 3 \times 10^{18}$ cm^{-2} (Cully et al. 1997). Col 6: photon flux ratio. Col 7: estimated electron density.

For the comparison of LETGS and HETGS spectra (Fig. 2) we proceeded as follows. First, we have fitted the relevant lines in the MEG and HEG spectra using the program CORA (Ness & Wichmann 2002); the smooth representation of each spectral region obtained with the above line fitting was converted to energy fluxes by use of the effective areas and exposure times, and finally rebinned to the resolution of the LETGS spectra; this procedure allows the proper overlay of the HETGS and LETGS data for ease of direct comparison.

Note that the line fitting is performed with a maximum likelihood method applied to the total source+background spectrum. In each spectral region the strongest lines are fitted with normalized Moffat profiles (Lorentzians with an exponent $\beta = 2.4$), representing the instrumental line spread function. The instrumental background is not subtracted from the total measured spectrum, but is instead added to the model spectrum consisting of the sum of all line emission components. The line counts are obtained as normalization factors of the line profiles.

Figure 2 shows the HETGS vs. LETGS (October 2000) comparison for the Si XIII and Ne IX triplets; the original HETGS/MEG spectrum in the region of Ne IX is also shown. What is immediately evident is the excess emission at the positions of the Si XIII and Ne IX intercombination lines (6.69 Å and 13.55 Å, respectively) in the LETGS spectrum with respect to the HETGS case. No such enhancement is visible in the O VII (21.6, 21.8, 22.1 Å) and Mg XI (9.17, 9.23, 9.31 Å) triplets (not shown); note that the latter is affected by low signal to noise ratio because of the relatively low Mg abundance in the corona of AD Leo (Maggio et al. 2004).

We have verified that the above enhancements are still visible, although somewhat reduced, also in the last 32 ks of the October 2000 observations, i.e. where the X-ray emission is again at its quiescent level. Some enhancement is also visible in the Ne IX intercombination line of the January 2000 LETGS spectrum, although the shorter exposure time makes the signal to noise ratio too low for any robust indication.

We have also carefully re-examined the long-wavelength ($\lambda > 100$ Å) region of the LETGS spectrum, for evidence of density-sensitive Fe XXI lines; in particular, we have searched the lines listed in Table 1, and measured total counts or upper limits, as appropriate. We confirm the detection of the strong 128.7 Å line (Fig. 2), and also of weaker spectral features at λ 102.2, 121.2, and 145.65 Å, already tentatively identified by

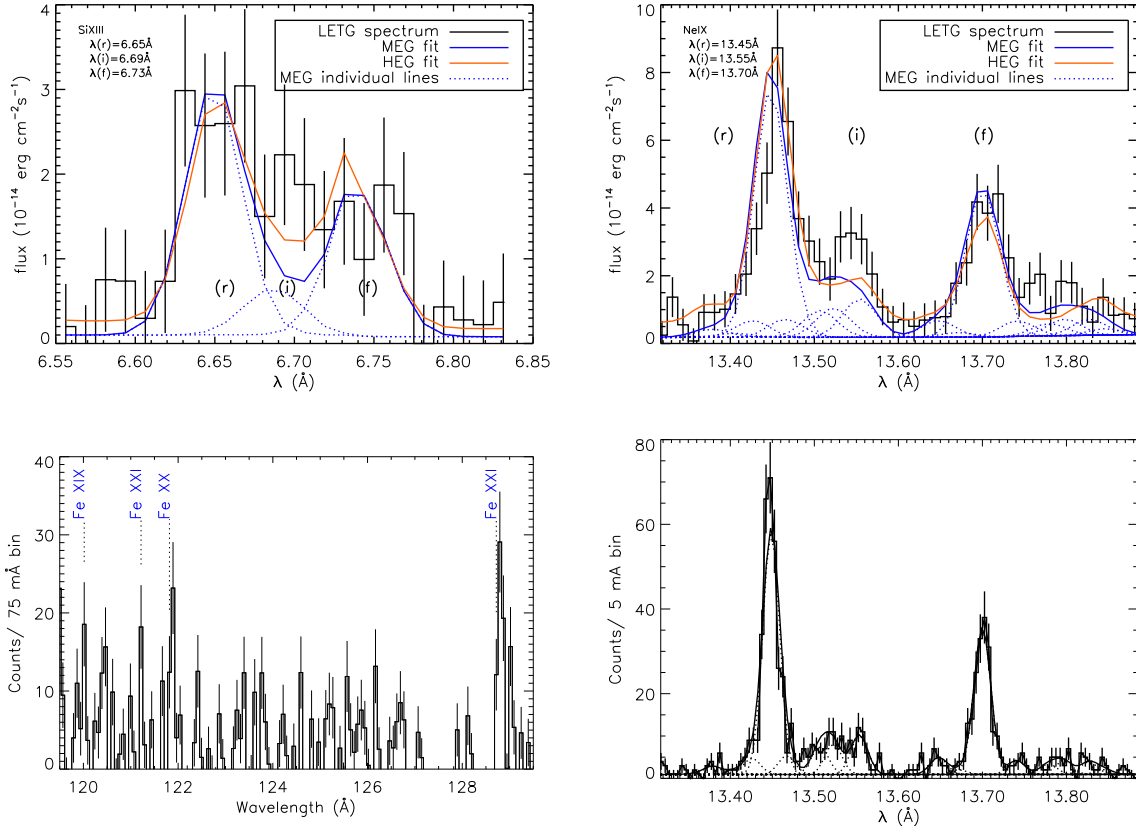


FIG. 2.— Upper panels: LETG Si XIII and Ne IX triplets compared with scaled HETGS line fitting models. Lower left: LETG spectral region including Fe XXI lines at 121.2Å and 128.7Å. Lower right: Ne IX triplet in the MEG spectrum of AD Leo, with 18 best-fit line components.

Maggio et al. (2004). Unfortunately, all the latter three features are characterized by quite a low S/N ratio ($2-3\sigma$), and there are residual uncertainties in the wavelength calibration of the LETGS that suggest caution in their identification; they fall at the nominal position of density-sensitive Fe XXI lines, and we will treat them as such in the following. The densities (or upper limits) implied by these diagnostics were estimated from the predicted line ratios (Fig. 3), according to APED (Plasma Emission Database V1.3, Smith et al. 2001); all the observed ratios, properly corrected for the instrument effective area and ISM absorption factor, consistently indicate a density N_e in the range $10^{12.0}-10^{12.2} \text{ cm}^{-3}$, within statistical uncertainties, with the exception of the 117.51/128.73 ratio. Note that the non-detection of the 117.51 Å line is puzzling, because this line is predicted to be relatively strong and very weakly dependent on the electron density, hence we suspect that its theoretical emissivity is overestimated.

It is more difficult to measure the Fe XXI line fluxes at short wavelengths because the spectral region 12.2–12.6 Å is especially crowded with hundreds of relatively faint iron lines, mostly from Fe XIX–XXII. In particular, we have searched for the density-sensitive lines at 12.284 Å, and 12.327 Å. The former has the highest emissivity at densities below $N_e \approx 10^{12.7} \text{ cm}^{-3}$ and it is clearly present in all X-ray spectra we have analyzed, while the second line is expected to become enhanced only in the high-density regime, above $N_e \approx 10^{12.4} \text{ cm}^{-3}$, and it is not convincingly detected in any of the spectra.

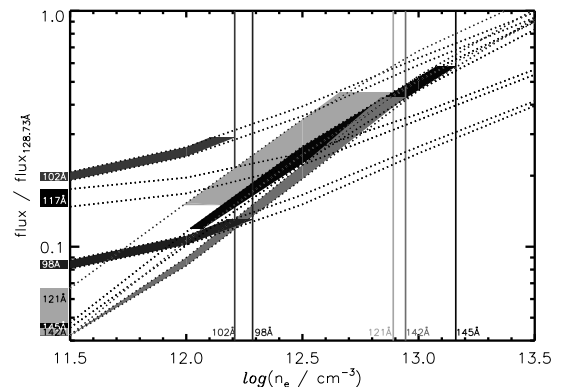


FIG. 3.— Fe XXI predicted density-sensitive Fe XXI line ratios, for the temperature range $10^{6.8}-10^{7.2} \text{ K}$ (lower and upper borders). The shaded areas indicate the density ranges consistent with the data; the vertical lines are placed at the high-density limits.

4. DISCUSSION AND CONCLUSIONS

The measurement of coronal plasma densities by means of X-ray spectral diagnostics is a difficult task (see §1). For example, the Ne IX triplet is heavily blended with Fe XIX lines, and to a lesser extent with Fe XX–XXI lines. A detailed analysis of this spectral region in *Chandra* and XMM-Newton spectra of Capella (Ness et al. 2003) showed that APED is sufficiently accurate and complete that all significant observed

lines in this region can be reasonably identified in the *Chandra*/HEG spectra, but spectra at lower resolution may be inadequate to derive reliable results. In fact, independent analyses of the Ne IX triplet in the same (October 2000) LETGS spectrum of AD Leo, performed by Ness et al. (2002) and by Maggio et al. (2004), resulted in quite different estimates of the plasma density owing to the different treatment of blends by these authors.

An apparent inconsistency emerges also by comparing the results in Maggio et al. (2004) and in the recent work by Ness et al. (2004), who included the *Chandra*/HETGS observation of AD Leo in a large sample of grating spectra of stellar coronae. While the former paper reports densities $N_e \sim 4 \times 10^{11} \text{ cm}^{-3}$ at $T \sim 10^{6.6} \text{ K}$ (peak emissivity temperature of the Ne IX) and $N_e \sim 2 \times 10^{12} \text{ cm}^{-3}$ at $T \sim 10^7 \text{ K}$ (Fe XXI), no evidence of especially high densities appears in the survey by Ness et al. (2004).

The present investigation resolves this issue; the direct comparison of the LETGS and HETGS spectra of AD Leo suggests that the star was observed in different coronal emission regimes, a high-density state in October 2000 and a low-density state in June 2002. The high density is strongly supported by the enhanced flux observed at the positions of the intercombination lines of the Ne IX and Si XIII He-like triplets; our investigation of density-sensitive Fe XXI lines in the October 2000 LETGS spectrum appears to be consistent with the above conclusion, although there remain uncertainties in the identification of some of these lines. Note that densities of a few $\times 10^{12} \text{ cm}^{-3}$ in the corona of AD Leo have already been reported by Sanz Forcada & Micela (2002), based on EUVE spectra.

The above picture is not entirely clear for two reasons; first, a density increase should affect both the intercombination (*i*) line and the forbidden (*f*) line in each He-like triplet, while we see only an enhancement of the *i* line; secondly, the temperature-sensitive ratios $G(T) = (i+f)/r$, with *r* denoting the resonance line, is significantly higher in the October 2000 LETGS spectrum than in the HETGS spectrum, with the consequence that, apparently, the plasma temperature was lower in the high-density state, a result which is difficult to understand. Since the Ne IX *i* line is strongly blended with Fe XIX, which forms at a higher temperature ($T \sim 10^{6.9} \text{ K}$), we have checked whether the enhancement of the *i* line could be explained by a contamination effect; none of the strongest lines from other comparably hot ions appears to be significantly different in the two spectra, and hence we have no reason to suspect an increased Fe XIX line emission in the Oct 2000 corona of AD Leo. Another possibility is that of a cooling plasma in which the population of the $1s2p \ ^3P$ levels (and hence the *i* line) is preferentially enhanced with respect to the 3S level (*f* line) in case of strong recombination effects; however, the expected recombination time scales are much shorter

than the observation length, hence a continuous replenishment of plasma is required to explain our finding. We conclude that the temperature indicated by the Ne IX $G(T)$ ratio is not reliable, for reasons yet to be understood.

Another puzzling result comes from the comparison of the O VII triplet in the different observations: contrary to naive expectation, the density-sensitive f/i ratio turns out to be significantly higher in October 2000 than in June 2002 (3.2 ± 0.6 vs. 1.9 ± 0.6 , respectively), indicating a lower density in the first case ($\log N_e = 9.9 \pm 0.7$ and $10.5 \pm 0.3 \text{ cm}^{-3}$, respectively). Instead, the temperature-sensitive $G(T)$ ratios are in perfect agreement, and they always indicate an “effective” formation temperature of $\approx 2 \times 10^6 \text{ K}$, i.e. coincident with the O VII emissivity maximum. Again, this is not easy to explain, because the plasma emission measure distribution vs. temperature in the corona of AD Leo peaks at $\approx 8 \text{ MK}$, and hence one expects an important contribution to the O VII line emission coming from plasma at temperatures higher than 2 MK. This anomalous behavior of the $G(T)$ ratios was also noted in the survey of coronal densities by Testa et al. (2004).

In conclusion, our detailed comparison of the different *Chandra* observations of AD Leo indicates that the plasma density in the corona of this active star may change substantially. The coincidence of the observed density enhancement with a higher X-ray emission level is suggestive of a dynamic phenomenon, possibly related to flaring activity. However, the observed variability of the X-ray emission can be due also to active regions in the stellar corona coming in and out of sight, due to rotational modulation, or due to the natural lifetime of the magnetic fields which provide confinement and heating of the plasma. For this reason, a significant variation of the temperature may not occur.

In any case, the interpretation of widely used spectral diagnostics, such as the He-like triplets or Fe XXI density-sensitive lines is certainly complicated by the likely existence of density inhomogeneities in the coronal plasma, besides obvious uncertainties in the atomic physics and in our ability to resolve all the relevant spectral components with the available data. In fact, as already pointed out by Güdel (2004), the observed line ratios may not describe “local densities” but rather the steepness of the density distribution with temperature. In this respect, predictions of the coronal X-ray spectra, taking into account physically realistic distributions of the magnetic structures, would be the next step in achieving progress in stellar coronal physics and X-ray spectroscopy.

AM acknowledges partial support from Ministero dell’Università e della Ricerca Scientifica. JUN acknowledges support from PPARC under grant number PPA/G/S/2003/00091. We also thank C. Jordan and P. Testa for helpful discussions and comments.

REFERENCES

- Audard, M., Güdel, M., Drake, J. J., & Kashyap, V.L. 2000, ApJ, 541, 396
 Cully, S., Fisher G., Hawley S. L., & Simon T. 1997, ApJ, 491, 910
 Favata, F., Micela, G., & Reale, F. 2000a, A&A, 354, 1021
 Güdel, M. 2004, A&A Rev., 12, 71
 Güdel, M., Audard, M., Skinner, S. L., & Horvath, M. I. 2002, ApJ, 580, L73
 Ness, J.-U., Brickhouse, N., Drake, J. J., & Huenemoerder, D. P. 2003, ApJ, 598, 1277
 Ness, J.-U., Schmitt, J. H. M. M., Burwitz, V., Mewe, R., Raassen, A. J. J., van der Meer, R. L. J., Predehl, P., & Brinkman, A. C. 2002, A&A, 394, 911
 Ness, J.-U., Güdel, M., Schmitt, J. H. M. M., Audard, M., & Telleschi, A. 2004, A&A, 427, 667
 Ness, J.-U., & Wichmann, R. 2002, Astronomische Nachrichten, 323, 129
 Maggio, A., Drake, J. J., Jr., Kashyap, V. L., Harnden, F. R., Jr., Micela, G., Peres, G., & Sciortino, S. 2004, ApJ, 613, 548
 Sanz Forcada, J., & Micela, G. 2002, A&A, 394, 653
 Smith, R. K., Brickhouse, N. S., Liedahl, D. A., & Raymond, J. C. 2001, ApJ, 556, 91
 Spiesman, W. J., & Hawley, S.L. 1986, AJ, 92, 664
 Testa, P., Drake, J. J., & Peres 2004, ApJ, in press
 van den Besselaar, E. J. M., Raassen A. J. J., Mewe, R., van den Meer, R. L. J., Güdel, M., Audard M. 2003, A&A, 411, 587
 Weisskopf, M. C., Brinkman, B., Canizares, C., Garmire, G., Murray, S., & Van Speybroeck, L. P. 2002, PASP, 114, 1